Crystal Structure of Two Ternary Complexes of Phosphorylating Glyceraldehyde-3-phosphate Dehydrogenase from Bacillus stearothermophilus with NAD and d-Glyceraldehyde 3-Phosphate

Claude Didierjean, Catherine Corbier, Mustapha Fatih, Frederique Favier, Sandrine Boschi-Muller, Guy Branlant, André Aubry

THE JOURNAL OF BIOLOGICAL CHEMISTRY
Vol. 278, No. 15, Issue of April 11, pp. 12968–12976, 2003

Printed in U.S.A.

Crystal Structure of Two Ternary Complexes of Phosphorylating Glyceraldehyde-3-phosphate Dehydrogenase from *Bacillus stearothermophilus* with NAD and D-Glyceraldehyde 3-Phosphate*

Received for publication, October 29, 2002, and in revised form, January 30, 2003
Published, JBC Papers in Press, February 4, 2003, DOI 10.1074/jbc.M211040200

Claude Didierjean‡, Catherine Corbier‡, Mustapha Fatih‡, Frédérique Favier‡, Sandrine Boschi-Muller§, Guy Branlant§¶, and André Aubry‡‖

From the ‡Laboratoire de Cristallographie et de Modélisation des Matériaux Minéraux et Biologiques, Groupe Biocristallographie, UMR 7036, CNRS-Université Henri Poincaré, Faculté des Sciences, 54506 Vandoeuvre Cedex, France and §Maturation des ARN et Enzymologie Moléculaire, UMR 7567, CNRS-UHP, Faculté des Sciences, 54506 Vandoeuvre Cedex, France

The crystal structure of the phosphorylating glyceraldehyde-3-phosphate dehydrogenase (GAPDH) from *Bacillus stearothermophilus* was solved in complex with its cofactor, NAD, and its physiological substrate, D-glyceraldehyde 3-phosphate (D-G3P). To isolate a stable ternary complex, the nucleophilic residue of the active site, Cys^{149}, was substituted with alanine or serine. The C149A and C149S GAPDH ternary complexes were obtained by soaking the crystals of the corresponding binary complexes (enzyme·NAD) in a solution containing G3P. The structures of the two binary and the two ternary complexes are presented. The D-G3P adopts the same conformation in the two ternary complexes. It is bound in a non-covalent way, in the free aldehyde form, its C-3 phosphate group being positioned in the P_s site and not in the P_i site. Its C-1 carbonyl oxygen points toward the essential His^{176}, which supports the role proposed for this residue along the two steps of the catalytic pathway. Arguments are provided that the structures reported here are representative of a productive enzyme·NAD·D-G3P complex in the ground state (Michaelis complex).

Phosphorylating glyceraldehyde-3-phosphate dehydrogenases (GAPDH)[1] are tetrameric enzymes that catalyze reversibly the oxidative phosphorylation of D-glyceraldehyde 3-phosphate (D-G3P) into 1,3-diphosphoglycerate (1,3-dPG) in the presence of cofactor NAD(P) via a two-step chemical mechanism. This mechanism has been well documented for the homotetrameric GAPDHs involved in glycolysis (1). First, the acylation step leads to the formation of a thioacylenzyme intermediate and NADH. This step includes: 1) the binding of D-G3P to the binary complex GAPDH·NAD; 2) the formation of a covalent thiohemiacetal intermediate with D-G3P; and 3) the hydride transfer from the thiohemiacetal intermediate toward the C-4 position of the nicotinamide ring of NAD. Second, the phosphorylation step consists of a nucleophilic attack of inorganic phosphate toward the thioacylenzyme intermediate that leads to formation of 1,3-dPG. This step, which is rate-limiting, includes the binding of inorganic phosphate to the enzyme intermediate, possibly preceded by an isomerization step consisting of a replacement of NADH by NAD (2).

Two amino acids are essential for the chemical mechanism, Cys^{149} and His^{176}. The high catalytic efficiency of GAPDHs toward D-G3P implies prerequisites with respect to the chemical mechanism. First, Cys^{149} should be in a thiolate form within the ternary Michaelis complex to efficiently attack the C-1 aldehydic group of D-G3P. This is ensured in part through the formation of an ion pair with His^{176}, which decreases Cys^{149} pK_{app} from 8.0 to 5.9 (3). Second, the hydride transfer should be efficient. This is assisted by His^{176}, which plays the role of a base catalyst. Moreover, the different intermediates and transition states, including the Michaelis complex, GAPDH·NAD·D-G3P, and the thioacylenzyme intermediate, should be stabilized within the active site. This is likely another role for His^{176} (Fig. 1).

The chemical nature of the substrates, G3P and inorganic phosphate, and the product, 1,3-dPG, implies the presence of two anion recognition sites in GAPDHs. These two anion binding sites have been tentatively identified within the active site from the location of two sulfate ions coming from the crystallization medium (4). On the basis of model building of the lobster GAPDH thiohemiacetal intermediate, these two anion binding sites were postulated to correspond to those binding the C-3 phosphate group of D-G3P (P_s site) and the inorganic phosphate ion (P_i site) (4). In all bacterial and eukaryotic GAPDHs, the P_s site is composed of the side chains of residues Arg^{231} and Thr^{179} and the 2′-hydroxyl group of the nicotinamide ribose when NAD is bound; the P_i site includes the side chains of residues Ser^{148} and Thr^{208} and the main chain nitrogen of Gly^{209}.

The P_s site has been found to occupy an identical location in all the crystal structures of eukaryotic and bacterial GAPDHs solved so far (4–14). But, the "true" location of the P_i site remains a matter of debate. Indeed, depending on the considered structure, the β-strand-loop-α helix segment containing residues 206–210 (called loop 206–210) has been observed in two different conformations, giving rise to two alternative lo-

* This work was supported by the Centre National de la Recherche Scientifique, the French Ministère de la Recherche et de l'Enseignement Supérieur, and local funds from the Région Lorraine. The costs of publication of this article were defrayed in part by the payment of page charges. This article must therefore be hereby marked "*advertisement*" in accordance with 18 U.S.C. Section 1734 solely to indicate this fact.

The atomic coordinates and structure factors (code 1NPT, 1NQ5, 1NQA, and 1NQO) have been deposited in the Protein Data Bank, Research Collaboratory for Structural Bioinformatics, Rutgers University, New Brunswick, NJ (http://www.rcsb.org/).

¶ To whom correspondence may be addressed. Tel.: 33-3-83-68-43-04; Fax: 33-3-83-68-43-07; E-mail: guy.branlant@maem.uhp-nancy.fr.

‖ To whom correspondence may be addressed. Tel.: 33-3-83-68-48-69; Fax: 33-3-83-40-64-92; E-mail: aubry@lcm3b.uhp-nancy.fr.

[1] The abbreviations used are: GAPDH, glyceraldehyde-3-phosphate dehydrogenase; G3P, glyceraldehyde 3-phosphate; 1,3-dPG, 1,3-diphosphoglycerate; PEG, polyethylene glycol.

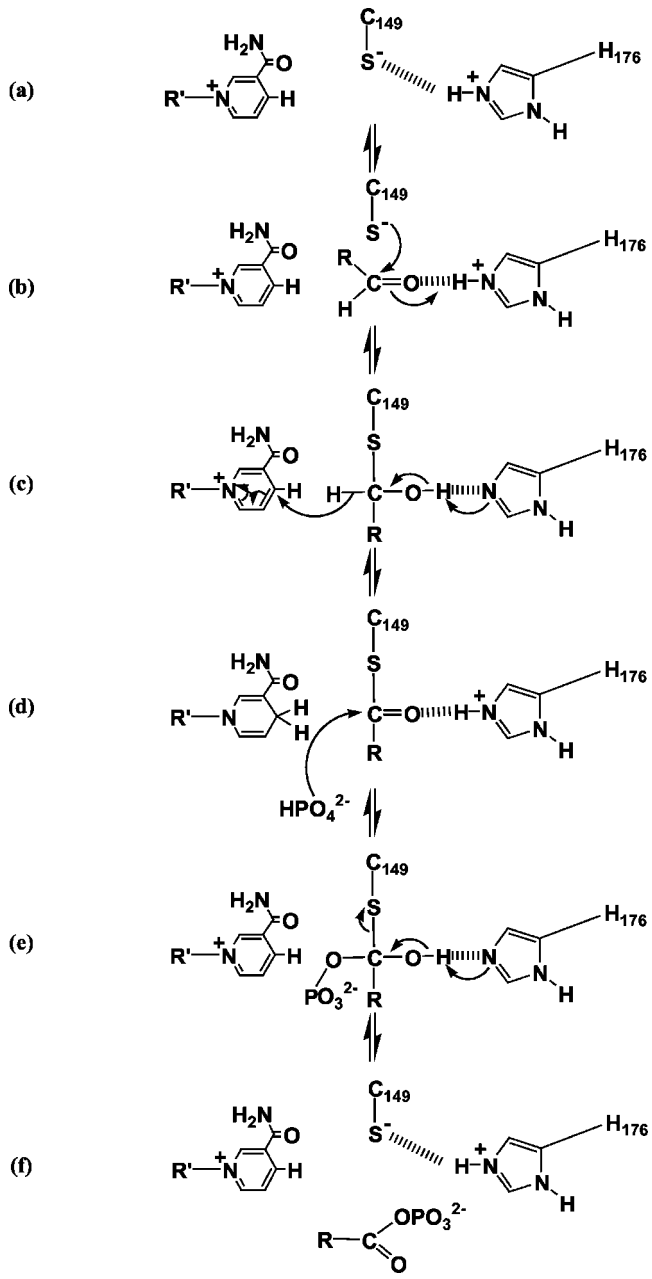

FIG. 1. **Schematic representation of the postulated catalytic mechanism of phosphorylating GAPDHs.** The catalytic mechanism can be divided into two steps. In the acylation step, Cys^{149} and His^{176} form an ion pair in holo-GAPDH (*a*). This decreases the pK_{app} of Cys^{149}, thus facilitating the thiolate attack toward the C-1 of D-G3P. The role of His^{176} is also to stabilize the binding of the substrate in the Michaelis complex GAPDH·NAD·D-G3P (*b*), the thiohemiacetal intermediate (*c*), and the thioacylenzyme intermediate (*d*). His^{176} also plays a role as a base catalyst facilitating the hydride transfer from the thiohemiacetal toward the nicotinamidium of NAD (*c*). In the phosphorylating step, the binding of inorganic phosphate to the thioacylenzyme is followed by its nucleophilic attack toward the thioacyl intermediate (*d*), which leads *via* a sp^3-phosphorylated intermediate (*e*) to the formation and release of 1,3-dPG (*f*). His^{176} is postulated to stabilize the tetrahedral intermediate (*e*) and to facilitate, as an acid (*d*) or base (*e*) catalyst, the 1,3-dPG formation. The exchange cofactor step, which consists of NADH release prior to NAD and inorganic phosphate binding, remains controversial (32–40). *R′* represents the adenine-ribose-phosphate-phosphate-ribose part of the cofactor, NAD. *R* represents the $CH(OH)COPO_3$ part of the substrate, D-G3P.

cations for the P_i site. The most common conformation is the one found in the holoenzyme from *Bacillus stearothermophilus* (7), whereas a second conformation is observed for instance in the holostructure from *Leishmania mexicana* and generates a P_i site that is located closer to the catalytic Cys^{149} residue and 2.9 Å away from the former position (9).

The contribution of the P_s and P_i sites during the two steps of the catalytic mechanism also remains a matter of debate. Taking into account the revised orientation of the side chain of His^{176} in the refined holostructure of *B. stearothermophilus* GAPDH, Skarzynski *et al.* (7) noticed that it was no longer possible to build a reasonable model of the hemithioacetal with its C-3 phosphate bound in the P_s site. They proposed that although the P_i site must be the location of the inorganic phosphate in the phosphorylation step, the C-3 phosphate of the substrate would bind first to the P_i site in the acylation step and then flip from the P_i site to the P_s site in the phosphorylation step. This hypothesis was supported by: 1) the inspection of the crystal structure of a ternary covalent complex, GAPDH·NAD·glycidol 3-phosphate, from *B. stearothermophilus*, which localizes the C-3 phosphate of the inhibitor within the P_i site (7); and also 2) kinetic analyses showing that substitution of Arg^{231} of the P_s site with glycine or leucine does not significantly affect the first-order rate constants of the overall oxidoreduction step (15), whereas mutations in the P_i site decrease this constant 4–7-fold (mutants T150A and T208A, respectively; see Ref. 16). The recent structure of a binary complex between *Escherichia coli* apoGAPDH and D-G3P, in which the C-3 phosphate group of the substrate is bound in the so-called "new P_i site," also supports this hypothesis (17).

In the present study, the crystal structures of two mutant GAPDHs from *B. stearothermophilus* in complex with the physiological substrate, D-G3P, have been determined at 2.0–2.2 Å resolution with the aim of evaluating the different hypotheses on the contribution of both P_s and P_i sites along the catalytic pathway. For this purpose, the active site Cys^{149} residue has been substituted by Ala and Ser. The C149A mutant GAPDH is inactive, whereas the C149S mutant GAPDH possesses a low residual activity (18). New crystallization conditions have been set up in the absence of any anions to avoid competitive binding with the C-3 phosphate of D-G3P. The structures presented here constitute the first example of ternary complexes mimicking the Michaelis complex, wild-type GAPDH·NAD·D-G3P. The results strongly suggest that the C-3 phosphate of D-G3P binds to the P_s site at least in the Michaelis ternary complex.

EXPERIMENTAL PROCEDURES

Site-directed Mutagenesis, Production, and Purification of Mutant B. stearothermophilus GAPDHs—Overexpression and purification of C149S mutant GAPDH were carried out by a procedure similar to that described earlier (18). For C149A mutant GAPDH, overexpression was carried out in *E. coli* HB101 strain (*supE44*, *hsdS20* (r^-, m^-), *recA13*, *ara-14*, *proA2*, *lacY1*, *galK2*, *rpsL20*, *xyl-5*, *mtl-1*) transformed with a pBluescriptII-derived plasmid containing the *gapA* gene of *B. stearothermophilus* under the control of the *lac* promoter. Site-directed mutagenesis was performed using the QuikChange site-directed mutagenesis kit (Stratagene). Purification of C149A mutant GAPDH was performed as described previously for other *B. stearothermophilus* mutant GAPDHs (3), except that a supplementary step was added to separate the *B. stearothermophilus* mutant GAPDH totally from the wild-type *E. coli* GAPDH produced by the HB101 cells. For this, enzyme solution was applied onto a phenyl-Superose HR column (Amersham Biosciences) equilibrated with Tris-HCl 50 mM, EDTA 2 mM, $(NH_4)_2SO_4$ 1.7 M, pH 8 buffer, followed by a linear gradient from 1.7 to 0.7 M $(NH_4)_2SO_4$. Under these conditions, C149A mutant *B. stearothermophilus* GAPDH was eluted at 1070 mM $(NH_4)_2SO_4$, and *E. coli* GAPDH at 850 mM.

Both mutant GAPDHs were isolated as apoforms, as judged by the A_{280}/A_{260} ratio of 2. The purity of the enzymes was checked by SDS-PAGE and mass spectrometry.

Activity Assay of GAPDH—Initial rate measurements were carried out at 25 °C on a Kontron Uvikon 933 spectrophotometer by following the absorbance of NADH at 340 nm. Thermostatted sample holders using a circulating water bath for all of the measurements maintained the temperature of the solutions at 25 °C. The experimental conditions

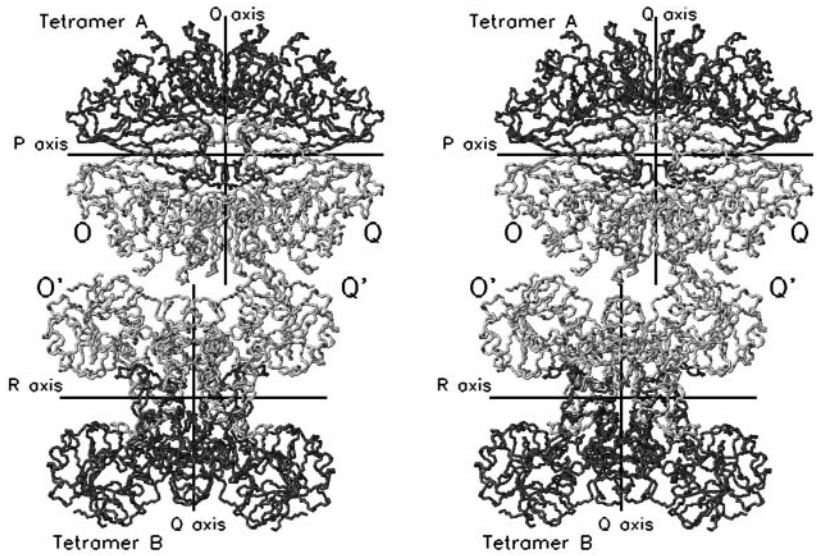

FIG. 2. **Crystal packing of the monoclinic form.** The two independent dimers of the asymmetric unit are represented in *gray*. Their symmetry-related dimers are shown in *black*. The symmetry operators (-x, y, 1-z) and (2-x, y, 1-z) were used to generate tetramers *A* and *B*, respectively. In this stereoview, the 2-fold crystallographic axis is vertical and corresponds to the *P* axis for tetramer A and the *R* axis for tetramer B.

were 1 mM, D,L-G3P and 1 mM NAD in 40 mM triethanolamine, 2 mM EDTA, 50 mM K_2HPO_4 buffer, pH 8.9. Protein concentrations were calculated using a molar extinction coefficient at 280 nm of $1.17.10^5$ M^{-1} cm^{-1}. Activities were expressed per monomer in s^{-1}.

Crystallization and Data Collection—Crystals of the binary complexes I and II (C149A GAPDH·NAD and C149S GAPDH·NAD) were obtained at 293 K using the hanging-drop vapor diffusion technique (19). Crystals of the C149A mutant protein were grown from a solution composed of 8% (w/v) polyethylene glycol (PEG) 4000, 0.1 M sodium acetate buffer, pH 4.6, 2 mM EDTA, 2 mM dithiothreitol, and 1.5 mM NAD, whereas the C149S mutant protein crystallized in quite similar conditions but in Tris-HCl buffer, pH 7.5, and with 10% (w/v) PEG 4000 as the precipitating agent.

Ternary complexes I and II (C149A GAPDH·NAD·D-G3P and C149S GAPDH·NAD·D-G3P) were obtained by soaking the crystals for 10 min in the crystallization solution containing 1.9 mM D,L-G3P. The crystals were then flash-frozen in liquid nitrogen by using 25% (v/v) 2-methyl-2,4-pentadiol as a cryoprotectant.

The four data sets were collected at 110 K on an area detector (DIP2030) with a Phi goniometer using CuKα radiation from a rotating anode generator (Model FR591, Nonius B. V.). The data sets were processed and scaled with the HKL suite (20). Binary complex I crystallized in space group $P3_121$ with one homotetramer/asymmetric unit. The crystal of the monoclinic binary complex II belongs to space group C2 and contains two independent dimers in the asymmetric unit (Fig. 2). The crystals of binary complex I and of ternary complex I diffracted to 2.2 Å resolution, whereas the crystals of binary complex II and ternary complex II diffracted to 2.1 and 2.0 Å, respectively. The statistics of the data sets are summarized in Table I.

Phasing and Refinement—The structure of the binary complexes were solved by molecular replacement (21) using the wild-type holostructure (Protein Data Bank code 1gd1) as the starting model and data from the 10 to 5 Å resolution range. Cycles of refinement (crystallography NMR software (CNS) (22)) alternated with manual rebuilding (TURBO-FRODO (23)) and inclusion of higher resolution data were carried out to improve the models.

Finally, the ordered water molecules were added. Each peak contoured at 3σ in the $F_o - F_c$ maps was identified as a water molecule, provided that hydrogen bonds would be allowed between this site and the protein. The models were then adjusted and refined up to a final convergence, using all of the reflections (sigma cut-off = 0.0) with *R* and *R*-free values of 17.7 and 21.0%, respectively, for the C149A binary complex and 19.8 and 24.9% for the C149S binary complex (Table I).

The ternary complexes were refined from the final models of the binary complexes using an identical procedure. The *R* and *R*-free values were 18.0 and 21.4%, respectively, for the C149A ternary complex and 19.3 and 23.5% for the C149S ternary complex (Table I).

Structure Analyses and Final Structure Parameters—The geometry of the models was checked with PROCHECK (24). Statistics concerning the geometry of the final models are given in Table I. All non-glycine residues are located in favorable regions of the Ramachandran plot (25), except Asp^{186} and Val^{237}, which belong to external loops and have side chains that are very well defined in the $(2F_o - F_c)$ density maps. The location of these residues outside the allowed regions has already been noticed in the crystal structures of GAPDHs isolated from other sources (11). The coordinates and the structure factors of the binary and ternary complexes have been deposited to the Protein Data Bank at Research Collaboratory for Structural Bioinformatics (ID codes 1NPT, 1NQ5, 1NQA, and 1NQO). Figs. 2–5 were drawn with MOLMOL (26) or TURBO-FRODO (23).

RESULTS

Biochemical Properties of Mutant GAPDHs—The *B. stearothermophilus* C149A mutant GAPDH was overproduced in *E. coli* cells, purified, and separated from the *E. coli* GAPDH by taking advantage of its lower hydrophobicity. This separation was accompanied by a drastic diminution of the activity from 5.10^{-4} s^{-1} to less than 1.10^{-6} s^{-1}. This result clearly shows that the C149A mutant GAPDH displays no significant dehydrogenase activity in contrast to the *E. coli* C149A mutant GAPDH, which was shown to display a significant non-phosphorylating activity (27). This finding suggests subtle structural differences between the active sites of *E. coli* and *B. stearothermophilus* GAPDHs (see below). On the other hand, the C149S mutant GAPDH displayed, as already published (18), a low but significant phosphorylating dehydrogenase activity with a k_{cat} of 8.10^{-3} s^{-1}.

Overall Structures—All GAPDH structures solved thus far share a common conserved fold composed of a NAD(P) binding domain and a catalytic domain. The enzyme is active as a homotetramer in which four subunits, designated O, P, Q, and R, are related by three perpendicular 2-fold axes, *P, Q*, and *R* (for nomenclature, see Ref. 28), with the choice of the first monomer for denomination "O" being arbitrary. Because the crystals of the wild-type holoenzyme from *B. stearothermophilus* (7) had been obtained in the presence of ammonium sulfate, which could have competed with the substrate for the binding to the anion recognition sites, new crystallization conditions had to be set up for the present study. Two new crystal forms have been obtained using PEG 4000 as the precipitant. The crystals of the binary complex C149A GAPDH·NAD (binary complex I) are trigonal and contain one typical homotetramer per asymmetric unit. The asymmetric unit of the monoclinic crystals obtained from the binary complex C149S GAPDH·NAD (binary complex II) is composed of two independent dimers (Fig. 2). Although having a different orientation, these two dimers are equivalent and were thus called OQ and O′Q′. Two biological tetramers (called A and B) were generated from these dimers OQ and O′Q′ by using the crystallographic 2-fold axis.

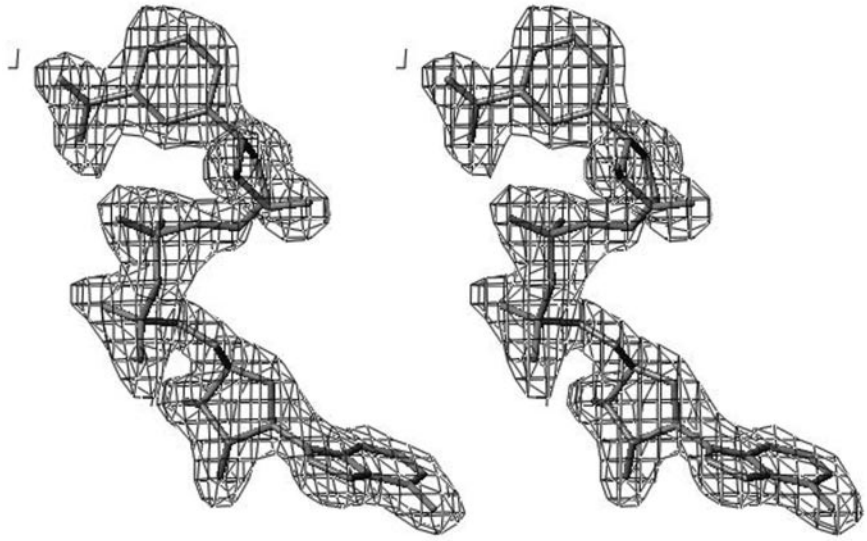

FIG. 3. **Stereoview of the final ($2F_o - F_c$) electron density map of the cofactor NAD$^+$.** This view corresponds to monomer O of ternary complex I (contour level, 1.2 σ).

In tetramer A, the crystallographic axis is along the 2-fold axis *P*, whereas in tetramer B, it corresponds to the *R* axis. A striking feature of this monoclinic form is the high compactness of the tetramers in the unit cell (Matthews coefficient, (V_M = 2.19 Å^3/Da)) when compared with the trigonal form (V_M = 2.92 Å^3/Da).

No significant structural differences are observed between the four monomers within each asymmetric unit. In the binary I and binary II complexes, the mean root-mean-square values obtained from the different pairwise superimpositions of the C_α atoms are 0.26 and 0.30 Å, respectively. For the ternary I and ternary II complexes, these values are 0.26 and 0.31 Å, respectively. In the four monomers of the binary or ternary complexes, the NAD molecule is well defined in the ($2F_o - F_c$) electron density maps (Fig. 3) and possesses average temperature factors similar to those of the protein (Table I).

Structure of the Binary Complexes: Comparison with the Wild-type Holoenzyme—Because the structure of the wild-type holoenzyme revealed a quasi-perfect 222 symmetry (7), the least-squares superimpositions involving the 334 C_α atoms of subunit O of the wild-type holoenzyme were realized with each subunit of the two binary complexes. The resulting root-mean-square differences are less than 0.45 Å, showing that the overall structures of the binary I and binary II complexes are very close to that of the wild-type holoenzyme. The largest differences mainly concern either solvent-exposed loops or regions involved in different contacts with symmetry-related molecules. In addition, differences can be noted for loop 206–210. This loop is located in the vicinity of the P_i site, which is "empty" in both the binary I and binary II complexes, whereas the side chain of Thr^{208} and the main chain nitrogen of Gly^{209} are directly involved in the binding of a sulfate anion in the structure of the wild-type holoenzyme (7). The displacement of residues 206–210 range from 0.2 to 1.1Å depending on the subunit. Furthermore, the average temperature factors calculated for all the atoms of the loop is 5 Å^2 higher than the average B-factor calculated for all the atoms of the subunit. These differences in B-values are not observed in the wild-type holostructure, in which the presence of the sulfate anion bound at the P_i site could stabilize the conformation of this loop. Nevertheless, the amplitude of the displacement remains small and insignificant when compared with that observed for the *E. coli* GAPDH·G3P binary complex (17). In the present work, the main conformation of loop 206–210 is rather similar to that observed in the structure of *B. stearothermophilus* wild-type GAPDH (7), as confirmed by omit maps (not shown) calculated in this region. Therefore, the P_i site must still be structurally competent to bind sulfate (or phosphate) even if the P_i site does not contain any sulfate anion in the mutant structures, because of the crystallization conditions used in this study. In both binary complexes, a broad electron density peak, identified as a sulfate ion, is observed within the P_s site. Because the crystallization trials have been conducted in the absence of sulfate, this anion arises most probably from the ammonium fractionation step of the purification and has not been eliminated despite the extensive dialyses carried out prior to the crystallization experiments.

Structures of the Ternary Complexes of Mutant GAPDHs—The comparisons of each ternary complex with its corresponding binary complex give root-mean-square differences of less than 0.12 Å showing that no significant conformational changes have been induced upon D-G3P binding. The analysis of the ($F_o - F_c$) maps of the two ternary complexes clearly revealed a peak of electronic density corresponding to the substrate D-G3P (Fig. 4).

The substrate adopts the same conformation in both structures and shares almost the same interactions with the enzyme (Table II). It is bound in a non-covalent way, its C-3 phosphate being positioned within the P_s site (Fig. 5), whereas the P_i site is devoid of density. The oxygen atoms of the C-3 phosphate group form hydrogen bonds with the conserved side chains of the residues Arg^{231} and Thr^{179} of the P_s site and with the 2′-hydroxyl group of the ribose adjacent to the nicotinamide of NAD (Table II, Fig. 5). In the holostructure of the wild-type enzyme (7), the nonconserved Arg^{195} residue of *B. stearothermophilus* GAPDH was also shown to interact with the sulfate anion at P_s site via a water molecule. This water molecule is present in the ternary complex I (WAT-440, see Table II) but is not found in the ternary complex II, although Arg^{195} occupies the same position as in the wild-type structure and in ternary complex I. Nevertheless, in both ternary complexes, the direct interactions shared between the phosphate group of the substrate and the protein are exactly the same as those observed for the sulfate ion occupying the P_s site in the holostructure of the wild-type enzyme (7).

Whereas D,L-G3P was used for the soaking experiments, the C-2 carbon adopts an *R* configuration, which accounts for the selective binding of the D-G3P, as expected because D-G3P is a better substrate than L-G3P (29). The C-2 hydroxyl group of D-G3P points toward the NH main chain of residue 149, with a distance of 3.6 Å between D-G3P-O-2 and Ser (or Ala)^{149} NH (Table II). The C-2 hydroxyl group also interacts with a water

TABLE I
Data collection and refinement statistics
Values in parentheses refer to the outermost resolution shell.

Crystal	Binary complex I	Ternary complex I	Binary complex II	Ternary complex II
Data collection				
Space group	$P3_121$	$P3_121$	C2	C2
a (Å)	115.7	115.6	140.48	140.31
b (Å)	115.7	115.6	87.91	87.84
c (Å)	224.8	223.9	119.92	119.41
β°			119.0	119.1
Z	6	6	4	4
Nominal resolution (Å)	2.18	2.2	2.11	2.01
Outermost resolution shell (Å)	2.26–2.18	2.28–2.2	2.18–2.11	2.07–2.01
Temperature (K)	110	110	110	110
Unique reflections	85949	83284	71736	77562
Completeness (%)	96.1 (91.)	96.3 (98.9)	99.2 (75.6)	92.8 (74.8)
R-merge[a]	0.061 (0.16)	0.065 (0.29)	0.085 (0.28)	0.105 (0.32)
Mean $I/\sigma(I)$	16.1 (5.2)	13.3 (3.7)	14.0 (3.4)	12.1 (3.2)
Refinement				
R-factor[b] (%)	17.7 (20.8)	18.0 (20.4)	19.8 (25.4)	19.3 (23.8)
R-free[c] (%)	21.0 (24.1)	21.4 (25.1)	24.9 (31.5)	23.5 (31.5)
r.m.s.d.[d] from ideal geometry				
Bond lengths (Å)	0.005	0.005	0.005	0.006
Bond angles (°)	1.4	1.4	1.4	1.4
Dihedral angles (°)	24.7	24.6	24.7	24.7
Improper angles (°)	0.84	0.83	0.90	0.86
Average B-factor (Å^2)				
Protein atoms	15.6	22.7	24.6	17.4
NAD	9.98	16.7	19.4	11.7
Sulfate	37.9		76.	
D-G3P		45.6		45.8
Water molecules	24.7	29.31	28.3	22.6

[a] *R*-factor for symmetry-related intensities.
[b] Crystallographic *R*-factor.
[c] *R*-factor for a randomly selected 10% of reflections not included in refinement.
[d] Root mean square deviation.

molecule (WAT-621) in the four monomers, which is stabilized through hydrogen bonding to the 2′O of the ribose adjacent to the nicotinamide ring (Fig. 5).

Although the equilibrium between the aldehyde and the gem-diol forms is strongly shifted in favor of the hydrated form in solution, analysis of the electron density allows us to conclude unambiguously that the substrate is bound under its reactive form (free aldehyde) within the active site, even for the C149A mutant GAPDH. This result correlates with the lack of activity of the *B. stearothermophilus* C149A mutant GAPDH but is nevertheless quite surprising, because the C149A mutant GAPDH from *E. coli* was shown to use the hydrated form as a substrate (27). Therefore, one could have expected to observe the gem-diol form bound into the active site in the case of the ternary complex I even at the pH of 4.6 of the crystallization medium. Some subtle differences in the active site between the *E. coli* and *B. stearothermophilus* C149A mutant GAPDHs probably account for this difference in behavior, which remains however unexplained because the residues composing the active site and their geometry are conserved in the two wild-type proteins (11). In the case of the ternary complex II of C149S mutant GAPDH, the lack of a covalent bond between D-G3P and Ser^{149} is consistent with the kinetic properties of the mutant protein. Indeed, the rate of the acylation step, of which the nucleophilic attack of Ser^{149} was shown to be rate-limiting, is decreased 10^5-fold compared with that of the k_{obs} of the wild type enzyme (18). In the crystallization medium, which contains PEG 4000, the acylation rate is probably decreased even more than in solution, which likely explains why, under the experimental x-ray conditions that include a flash-freezing after 10 min of soaking, the non-covalent ternary complex remains chemically stable within the crystal.

DISCUSSION

With the aim of better understanding the catalytic mechanism of GAPDH and of evaluating the hypothetical models deduced from kinetic and structural studies, we solved the crystal structure of the *B. stearothermophilus* GAPDH in complex with its physiological substrate, D-G3P. For this purpose, the active site nucleophilic residue, Cys^{149}, was substituted by alanine or serine. The mutant GAPDHs used herein are either inactive (Ala^{149}) or possess a low residual activity (Ser^{149}). New crystallization conditions have been set up in the absence of any anions in order to avoid competitive binding with the C-3 phosphate group of the substrate. The ternary complex structures have been solved and constitute the first example of a ternary complex, GAPDH·NAD·D-G3P. The substrate presents the same conformation in both structures. It is bound in a non-covalent way, under its aldehydic form, with its C-3 phosphate located in the P_s site. The binding of the C-3 phosphate group in the P_s site rather than in the P_i site is fully consistent with the observation that in the binary complexes, the P_s site was occupied with a sulfate ion coming from the purification step, whereas the P_i site was empty. This suggests a higher affinity of P_s site *versus* P_i site for phosphate and has been observed already in the structure of *B. stearothermophilus* wild-type enzyme. In this structure, the P_s site was fully occupied with sulfate coming from the crystallization medium, whereas the occupancy of the P_i site was only partial. These observations also support the hypothesis shared by Chakrabarti (30) and Copley and Barton (31) that the presence of an arginine residue within an anion binding site enhances its affinity for anions. In this regard, examination of the residues lining the P_s and P_i sites shows that Arg^{231} is involved in the formation of the P_s site, although no arginine residue contributes directly to the P_i site. Electrostatic potential calculations,

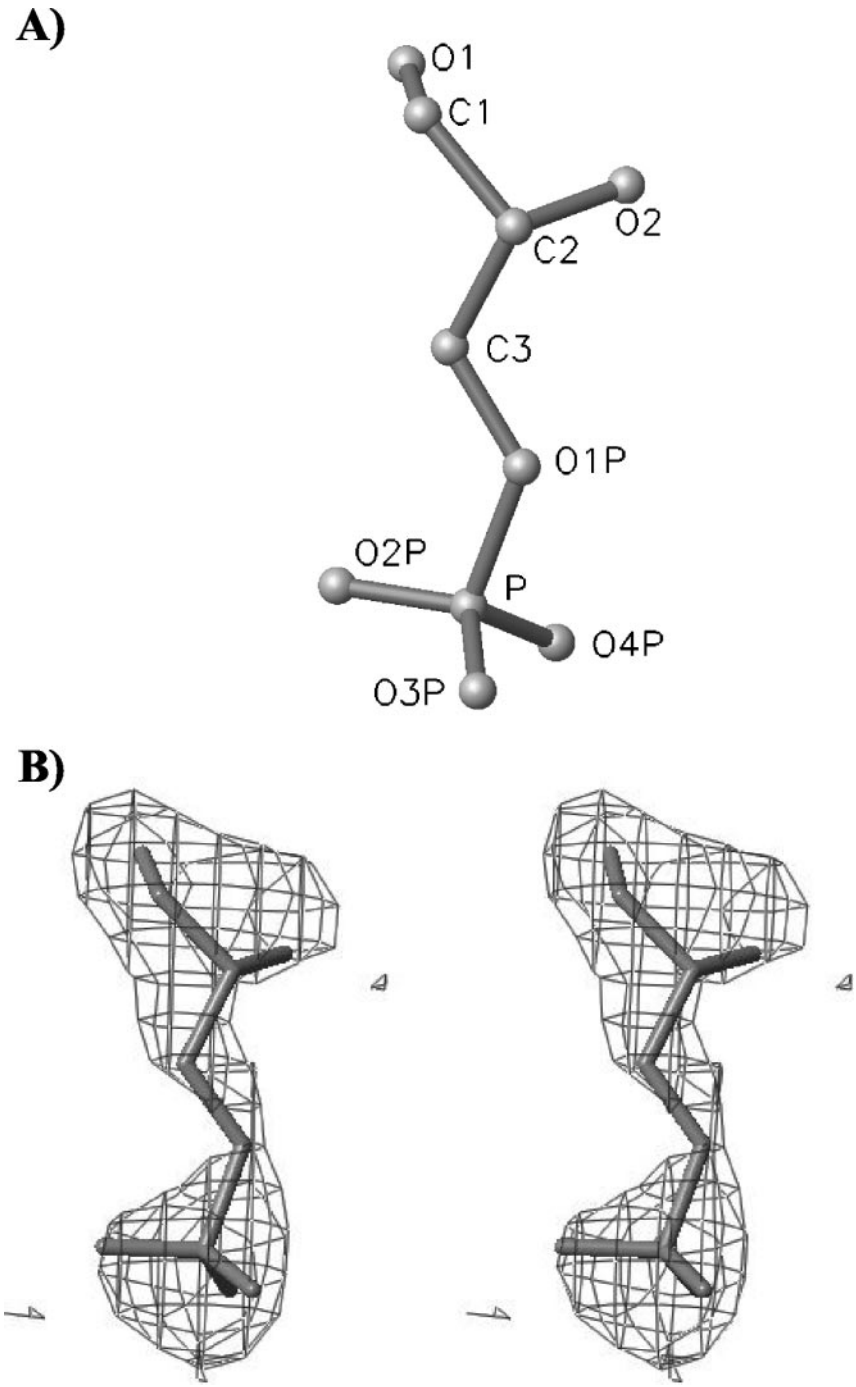

FIG. 4. **Views of the D-G3P molecule.** *A*, view of the D-G3P molecule with its atomic numbering scheme. *B*, stereoview of the D-G3P molecule in monomer O of ternary complex I shown in the (F_o – F_c) electron density calculated from the refined structure before the introduction of the substrate (contour level, 3 σ).

carried out on the monomer structure, confirmed that the local positive electrostatic potential is higher for P_s than for P_i sites (results not shown) and could explain the affinity differences between these two anion recognition sites.

Whereas a racemic mixture of G3P was used for the soaking experiments, only the D-enantiomer is bound. The molecular factors explaining this stereoselectivity of GAPDHs have been the subject of controversy in the literature. Modeling the hemithioacetal intermediate within the active site of the lobster enzyme led Moras *et al.* (4) to propose that the preference for the D-isomer could be explained by an interaction of the C-2 hydroxyl group of the substrate with the side chain of Ser^{148}. This hypothesis had been then refuted by Skarzynski *et al.* (7) who observed in the refined holostructure of *B. stearothermophilus* enzyme the presence of a hydrogen bond between the OH group of Ser^{148} and the main chain NH group of Thr^{151}, thus excluding the involvement of Ser^{148} in the stereoselectivity. More recently, Duée *et al.* (11) modeled the hemithioacetal intermediate in the crystal structure of *E. coli* GAPDH and proposed that an interaction between the O-2 atom (Fig. 4) and the NH group of Cys^{149} would explain this stereoselectivity. In our complexes, the side chain of Ser^{148} forms a hydrogen bond with the amide group of Thr^{151}, excluding any contribution of Ser^{148} to the stereoselectivity of substrate. The distance between the C-2 hydroxyl group of D-G3P and the NH group of residue 149 is consistent with the interpretation of Duée *et al.* (11). Furthermore, the interaction between the C-2–OH and a water molecule, stabilized through hydrogen bonding to the 2′O of the ribose adjacent to the nicotinamide ring (Fig. 5), might also contribute to the stabilization of the C-2 hydroxyl group.

In both ternary structures, the relative position of residue

TABLE II
Interactions between the substrate, D-G3P, and the active site residues

Distances are expressed in Å.

Ternary complex I (C149A mutant GAPDH)	O	P	Q	R
G3P-O4P—WAT-353	2.54	2.61	2.73	2.68
G3P-O4P—O2′N-NAD	3.12	3.14	3.19	3.19
G3P-O2P—T179-OG1	2.50	2.57	2.51	2.50
G3P-O2P—R231-NH2	2.76	2.89	2.70	2.82
G3P-O3P—WAT-440	2.92	3.21	2.99	2.80
G3P-O2—WAT-621	2.52	2.75	2.61	2.50
G3P-O2—A149N	3.58	3.60	3.39	3.70
G3P-O1—H176-NE2	2.83	2.69	2.74	2.79
Ternary complex II (C149S mutant GAPDH)	**O**	**Q**	**O′**	**Q′**
G3P-O4P—WAT-353	2.60	2.57	2.56	2.64
G3P-O4P—O2′N-NAD	3.01	3.33	3.01	2.98
G3P-O2P—T179-OG1	2.44	2.53	2.69	2.74
G3P-O2P—R231-NH2	2.64	2.74	2.66	2.64
G3P-O2—WAT-621	2.55	2.75	2.93	2.52
G3P-O2—S149N	3.46	3.64	3.66	3.60
G3P-O1—S149-OG	2.37	2.43	2.42	2.39
G3P-O1—H176-NE2	2.60	2.51	2.48	2.65

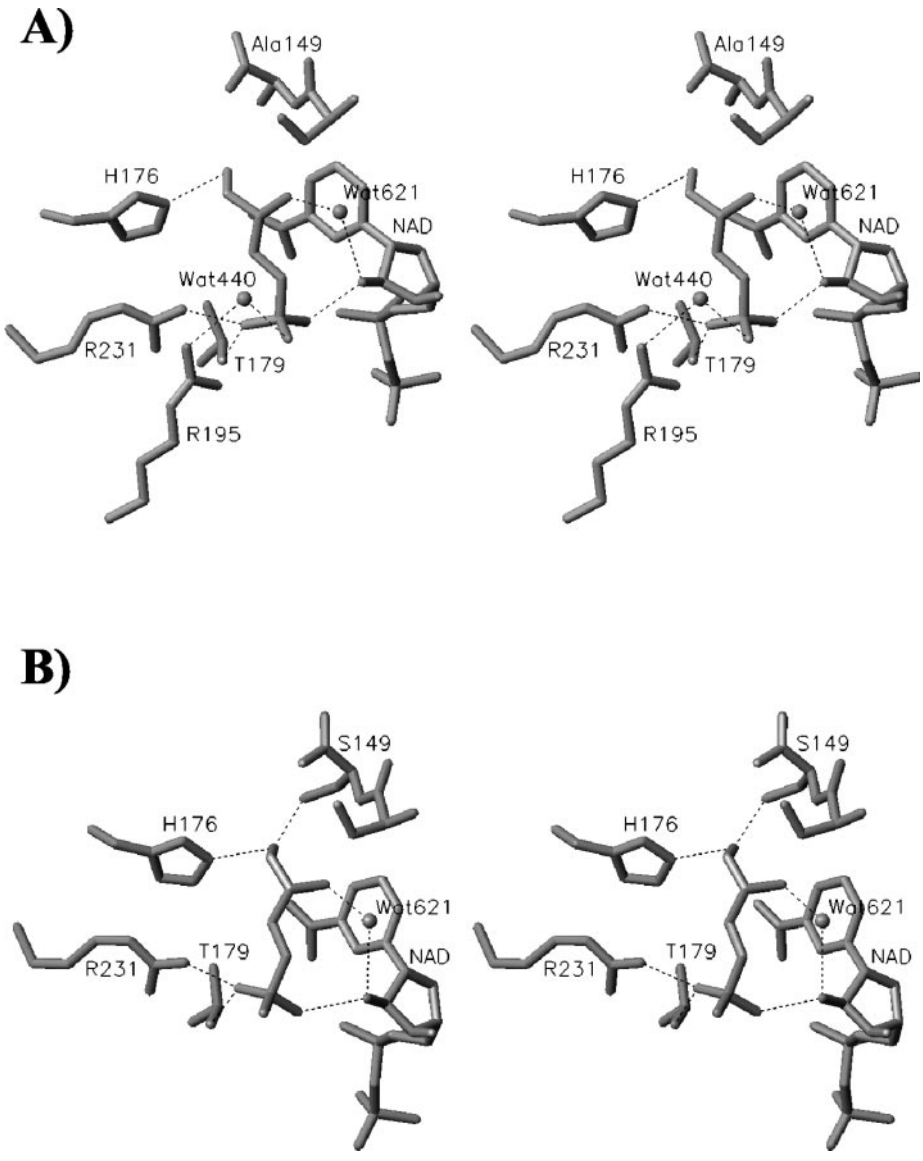

FIG. 5. **Stereoview of the active site in monomer O of the ternary complexes.** *A*, ternary complex I (C149A mutant GAPDH); *B*, ternary complex II (C149A mutant GAPDH). The residues that interact with the D-G3P molecule are labeled.

149 with respect to the C-1 atom of the substrate suggests that, assuming a similar positioning of Cys^{149}, the nucleophilic attack of Cys^{149} in the wild-type will occur on the Re face of the D-G3P. The O-1 oxygen of D-G3P is orientated for both mutant GAPDHs in such a way that it can accept a hydrogen bond from the $N_{\epsilon 2}$ atom of the catalytic His^{176} residue and also from the side chain of Ser^{149} for the ternary complex II (Table II). This is consistent with the role postulated for His^{176} in the stabili-

zation of the substrate (3) (Fig. 1). Altogether, our results suggest that the structures of the ternary complexes presented here are representative of the productive enzyme·NAD·substrate complex in the ground state (Michaelis complex). Indeed, the use of a C149S mutant GAPDH displaying a K_m value for D-G3P similar to that of the wild-type and the ideal orientation of the carbonyl O-1 oxygen with respect to the essential His^{176} residue let us suppose that the substrate is bound in a catalytically competent manner, analogous to the one it adopts in the Michaelis complex in the case of the wild-type enzyme.

These results, suggesting that the P_s site constitutes the binding site for the C-3 phosphate group of the substrate, are however a bit surprising because former structural studies carried out with the aim of obtaining a structure that mimics the hemithioacetal intermediate pointed to the involvement of the P_i site. Indeed, the structure of *B. stearothermophilus* holoenzyme in complex with a substrate analogue, glycidol 3-phosphate (7), as well as the structure of *E. coli* apoGAPDH in complex with D-G3P (17) both revealed that the C-3 phosphate group was located in the P_i site. From this point of view, the structures of the ternary complexes presented here are in apparent contradiction with the structural studies and the biochemical results mentioned in the Introduction. Several reasons, which are not mutually exclusive, can be put forward to explain this apparent discrepancy.

First, the structure of the *E. coli* enzyme in complex with D-G3P was carried out on the apoform (without NAD). It is, however, well established that NAD contributes to the formation of the P_s site (7), and therefore the lower affinity of a nonfunctional P_s site might explain why the C-3 phosphate was found in the P_i site in this structure. Furthermore, for this latter structure, Yun *et al.* (17) noticed that the C-1 hydroxyl group of D-G3P and the nicotinamide base would be close to each other and proposed that the positive charge of the nicotinamidium contributes to the stabilization of the tetrahedral transition intermediate. It was also observed that His^{176} was involved in the binding of the phosphate group of D-G3P and thus would be unable to play a role in stabilizing the tetrahedral intermediate and as a base catalyst for facilitating hydride transfer, which does not correlate with the conclusions drawn from former site-directed mutagenesis experiments (3).

Second, when compared now with the *B. stearothermophilus* GAPDH·NAD·glycidol 3-phosphate structure, the use of the true substrate of the enzyme in our ternary complexes shows that an H-bond is formed between the C-1 carbonyl and His^{176}-$N_{\epsilon 2}$, which could explain the different positioning of glycidol 3-phosphate. Indeed, the lack of oxygen atom at the C-1 position in the latter molecule prevents the formation of such an H-bond.

A third difference concerns the absence of a covalent link between the C-1 carbonyl atom and the catalytic residue Cys^{149} in our complex when compared with the two structures mentioned above.

In previous kinetic studies (15, 16), changing P_s site residues was shown to strongly decrease the k_{cat}, whereas changing P_i site residues led to moderate k_{cat} effects. In all mutant GAPDHs, the limiting step was shown to take place after the hydride transfer, and the K_m values of D-G3P were not drastically modified. The fact that changing P_i site residues decreased the first-order overall oxidoreduction rate, whereas changing P_s site residues did not, was interpreted as evidence in favor of an initial binding of the C-3 phosphate at the P_i site. Although it seems probable from the current structures that the P_s site in the wild-type enzyme constitutes the binding site for the C-3 phosphate group of the substrate in the non-covalent complex, GAPDH·NAD·D-G3P, our results do not rule out the possibility that the formation of the covalent bond between Cys^{149} and D-G3P promotes the repositioning of the C-3 phosphate in the P_i site before the hydride transfer. Modeling the hemithioacetal intermediate in the *B. stearothermophilus* wild-type enzyme (not shown) with the C-3 phosphate group positioned either in the P_s or in the P_i site leads to models equivalent to those already reported by Duée *et al.* (11) or Kim *et al.* (9). It is furthermore obvious from these modeling experiments that changing the position of the C-3 phosphate group from P_s site to P_i site requires only a rotation around the C-1–C-2 bond. This rotation can be achieved without significant changes in the position of the C-1 atom and, whatever the location of the C-3 phosphate group in either the P_s or P_i site, leads to a complex in which the relative position of His^{176} with respect to the C-1 hydroxyl group is consistent with the role of base catalyst proposed for His^{176}. Therefore, it is not possible to use these models to discriminate between the two alternative positioning for the C-3 phosphate group at the hemithioacetal intermediate level, except that binding in the P_s site seems to be more favorable from an energetic point of view, as already discussed by Kim *et al.* (9).

In conclusion, the structures of the ternary complexes presented here are probably representative of that of the wild-type enzyme·NAD·D-G3P ternary complex in the ground state. But it remains to be known whether the substrate will keep the same position, in particular with regard to its C-3 phosphate group, when the covalent bond within the ternary complex is formed between Cys^{149} and D-G3P. The fact that the thioacylenzyme intermediate can accumulate in the absence of phosphate could allow the determination of its crystal structure and thus the localization of the C-3 phosphate within one of the different covalent complexes formed along the catalytic mechanism.

Acknowledgments—We are very grateful to Dr. S. Azza for the production and purification of enzymes and to Drs. A. Van Dorsselaer and S. Sanglier-Cianferani for mass spectrometry analyses. We thank the Service Commun de Diffraction X sur Monocristaux (Université Henri Poincaré-Nancy 1) for providing access to crystallographic experimental facilities.

REFERENCES

1. Harris, J. I., and Waters, M. (1976) in *The Enzymes* (Boyer, P. D., ed) Vol. 13, pp. 1–49, Academic Press, New York
2. Harrigan, P. J., and Trenthan, D. R. (1974) *Biochem. J.* **143,** 353–363
3. Talfournier, F., Colloc'h, N., Mornon, J. P., and Branlant, G. (1998) *Eur. J. Biochem.* **252,** 447–457
4. Moras, D., Olsen, K. W., Sabesan, M. N., Buehner, M., Ford, G. C., and Rossmann, M. G. (1975) *J. Biol. Chem.* **250,** 9137–9162
5. Mercer, W. D., Winn, S. I., and Watson, H. C. (1976) *J. Mol. Biol.* **104,** 277–283
6. Griffith, J. P., Lee, B., Murdock, A. L., and Amelunxen, R. E. (1983) *J. Mol. Biol.* **169,** 963–974
7. Skarzynski, T., Moody, P. C. E., and Wonacott, J. A. (1987) *J. Mol. Biol.* **193,** 171–187
8. Vellieux, F. M. D., Hajdu, J., Verlinde, C. L., Groendijk, H., Read, R. J., Greenhough, T. J., Campbell, J. W., Kalk, K. H., Littlechild, J. A., Watson, H. C., and Hol, W. G. J. (1993) *Proc. Natl. Acad. Sci. U. S. A.* **90,** 2355–2359
9. Kim, H., Feil, I. K., Verlinde, C. L. M. J., Petra, P. H., and Hol, W. G. J. (1995) *Biochemistry,* **34,** 14975–14986
10. Korndörfer, I., Steipe, B., Huber, R., Tomschy, A., and Jaenicke, R. (1995) *J. Mol. Biol.* **246,** 511–521
11. Duée, E., Olivier-Deyris, L., Fanchon, E., Corbier, C., Branlant, G., and Dideberg, O. (1996) *J. Mol. Biol.* **257,** 814–838
12. Tanner, J. J., Hecht, R. M., and Krause, K. L. (1996) *Biochemistry* **35,** 2597–2609
13. Song, S., Li, J., and Lin, Z. (1998) *Acta Crystallogr. Sect. D Biol. Crystallogr.* **54,** 558–569
14. Souza, D. H. F., Garratt, R. C., Araujo, A. P. U., Guimaraes, B. G., Jesus, W. P. D., Michels, P. A. M., Hannaert, V., and Oliva, G. (1998) *FEBS Lett.* **424,** 131–135
15. Corbier, C., Michels, S., Wonacott, A. J., and Branlant, G. (1994) *Biochemistry* **33,** 3260–3265
16. Michels, S., Rogalska, E., and Branlant, G. (1996) *Eur. J. Biochem.* **235,** 641–647
17. Yun, M., Park, C. G., Kim, J. Y., and Park, H. W. (2000) *Biochemistry* **39,** 10702–10710
18. Boschi-Muller, S., and Branlant, G. (1999) *Arch. Biochem. Biophys.* **363,**

259–266
19. MacPherson, A. (1999) in *Crystallization of Biological Molecules,* pp. 165–167, Cold Spring Harbor Laboratory Press, New York
20. Otwinowski, Z,., and Minor, W. (1997) *Methods Enzymol.* **276,** 307–326
21. Navaza, J. (1994) *Acta Crystallogr. Sect. A* **50,** 157–163
22. Brünger, A. T., Adams, P. D., Clore, G. M., DeLano, W. L., Gros, P., Grosse-Kunsteleve, R. W., Jiang, J. S., Kuszewski, J., Nilges, M., Pannu, N. S., Read, R. J., Rice, L. M., Simonson, T., and Warren, G. L. (1998) *Acta Crystallogr. Sect. D Biol. Crystallogr.* **54,** 905–921
23. Roussel, P. A., and Cambillau, C. (1991) *TURBO-FRODO*, *Silicon Graphics Applications Directory*, Silicon Graphics, Mountain View, CA
24. Laskowski, R. A., MacArthur, M. W., Moss, D. S., and Thorton, J. M. (1993) *J. Appl. Crystallogr.* **26,** 283–291
25. Ramakrisknan, C., and Ramachandran, G. N. (1965) *Biophys. J.* **5,** 909–933
26. Koradi, R., Billeter, M., and Wuthrich, K. (1996) *J. Mol. Graph.* **14,** 51–55
27. Corbier, C., Della-Seta, F., and Branlant, G. (1992) *Biochemistry* **31,** 12532–12535
28. Buehner, M., Ford, G. C., Moras, D., Olsen, K. W., and Rossman, M. G. (1974) *J. Mol. Biol.* **82,** 563–585
29. Byers, L. D. (1978) *Arch. Biochem. Biophys.* **186,** 335–342
30. Chakrabarti, P. (1993) *J. Mol. Biol.* **234,** 463–482
31. Copley, R. R., and Barton, G. J. (1994) *J. Mol. Biol.* **242,** 321–329
32. Orsi, B. A., and Cleland, W. W. (1972) *Biochemistry* **11,** 102–109
33. Canellas, P. F., and Cleland, W. W. (1991) *Biochemistry* **30,** 8871–8876
34. Liu, L., and Huskey, W. P. (1992) *Biochemistry* **31,** 6898–6903
35. Segal, H. L., and Boyer, P. D. (1953) *J. Biol. Chem.* **204,** 265–272
36. Trentham, D. R. (1971) *Biochem. J.* **122,** 71–77
37. Dalziel, K., McFerran N. V., and Wonacott, A. J. (1981) *Philos. Trans. R. Soc. Lond. Biol. Sci.* **293,** 105–118
38. Duggleby, R. G., and Dennis, D. T. (1974) *J. Biol. Chem.* **249,** 167–174
39. Meunier, J. C., and Dalziel, K. (1978) *Eur. J. Biochem.* **82,** 483–492
40. Crow, V. L., and Wittenberger, C. L. (1979) *J. Biol. Chem.* **254,** 1134–1142

Crystal Structure of Two Ternary Complexes of Phosphorylating Glyceraldehyde-3-phosphate Dehydrogenase from *Bacillus stearothermophilus* with NAD and d-Glyceraldehyde 3-Phosphate

Claude Didierjean, Catherine Corbier, Mustapha Fatih, Frédérique Favier, Sandrine Boschi-Muller, Guy Branlant and André Aubry

J. Biol. Chem. 2003, 278:12968-12976.
doi: 10.1074/jbc.M211040200 originally published online February 4, 2003
